



# American Transactions on Engineering & Applied Sciences

<http://TuEngr.com/ATEAS>



## Analysis of Roll Rotation Mechanism of a Butterfly for Development of a Small Flapping Robot

Masahiro SHINDO <sup>a\*</sup>, Taro FUJIKAWA <sup>b</sup>, Koki KIKUCHI <sup>a</sup>

<sup>a</sup> Department of Advanced Robotics, Chiba Institute of Technology, JAPAN

<sup>b</sup> Department of Robotics and Mechatronics, Tokyo Denki University, JAPAN

### ARTICLE INFO

*Article history:*

Received July 24, 2014

Accepted July 31, 2014

Available online

August 01, 2014

*Keywords:*

CFD;

Flapping flight;

Roll rotation;

Posture control;

Aerodynamic characteristics.

### ABSTRACT

In this paper, we investigated the aerodynamic characteristics during roll rotation of a butterfly based on computational fluid dynamics using a three-dimensional high-speed camera information. This method allows to create a numerical model of a butterfly from the camera images and to analyze the flow field corresponding to the captured behavior. We photographed two behaviors different in rotational axis and analyzed the roll rotational mechanism. In a typical pitch rotational flight, the differential pressure was concentrated on the tip of fore wings. The magnitudes of reaction forces on left and right wings were roughly matched each other. On the other hands, the differential pressure of the roll rotational flight was distributed in the whole of wings. The magnitude of the right reaction force was twice greater than that of left at the first down stroke. The roll angle changed largely at the same time. These results show that a butterfly rotates about roll by changing the reaction forces on each side.

© 2014 Am. Trans. Eng. Appl. Sci.

## 1. Introduction

Birds and insects flap to achieve flight and can perform wonderful aerial feats such as vertical takeoff and landing, snap turns, and hovering. They gain high maneuverability by utilizing the vortices around the wings. A butterfly is a suitable model on which to base

\*Corresponding author (Masahiro Shindo). Email address: [s1376014we@s.chibakoudai.jp](mailto:s1376014we@s.chibakoudai.jp).

autonomous micro aerial vehicles (MAV), due to its sub-gram weight, low flapping frequency and a few degrees of freedom compared to other flying insects. To develop a small flapping robot, many studies on the flight mechanism of butterflies have been carried out (Wood 2011, 2013 and Shen 2012). Takahashi *et al.* have developed a micro strain sensor using micro electronic mechanical systems (MEMS) and measured the pressure by mounting it on the wings (Takahashi, 2012). The result of measurement showed that the differential pressure on the fore wings was dominant over the pressure on the hind wings. However, in this experiment, the butterfly flew while pulling a signal wire because the sensor was physically connected to an external circuit board. Therefore, it is possible that the flight behavior was different to that of an untethered butterfly. Fuchiwaki *et al.* have visualized vortices around two kinds of butterfly using particle image velocimetry (PIV) (Fuchiwaki, 2013). The results show that a vortex ring is formed at the beginning of the down stroke and passes over the body with growing vortices and flow speed regardless of the type of a butterfly. The PIV method is able to analyze the air flow in an arbitrary plane in space; however, flapping is a complex 3D action which requires the 3D visualization of vortices.

We clarify the attitude recovering mechanism of a butterfly by analyzing an untethered butterfly and visualizing the pressure and vortices. We photograph the flapping behavior using a 3D high speed camera system. The 3D data from different points on the butterfly wings are obtained from all three directions. The attitude (roll, pitch, and yaw angles) and flapping angle are determined by using these points. These points and velocities are also used as the boundary conditions for computational fluid dynamics (CFD). By reproducing the actual behavior of a butterfly in a computer, the airflow around the measured points can be deduced. Based on this numerical procedure, the magnitude and distribution of pressure and the behavior of the vortices can be visualized. Accordingly, the lift and drag forces on the butterfly are calculated by considering the pressure over the whole wing. This study clarifies the roll rotation mechanism of a butterfly by determining the reaction force exerted and the angular moments during flight.

## 2. Photography of Flight Behavior

### 2.1 Analysis of the Images

In this study, we photographed the free flight behavior of *Papilio xuthus* using a 3D high speed camera system (Figure 1). The camera coordinate system has three axes parallel to the

camera directions and its origin is fixed at the takeoff point of the butterfly. All cameras are orthogonally located 1,500mm from the roost. Table 1 shows the photography parameters. The captured space is  $250 \times 250 \times 250 \text{ mm}^3$ . The positions of the cameras are identified by calibration using a target, and then the coordinates of the measured points are calculated using epipolar geometry.

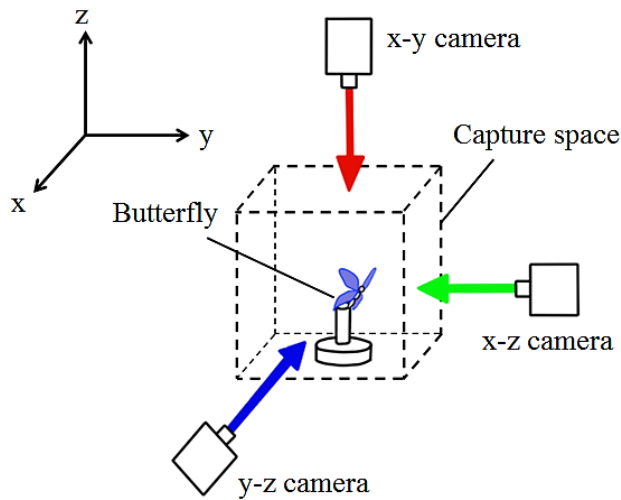


**Figure 1:** Camera configuration.

**Table 1:** Camera parameter.

Frame rate	1000 frame/sec
Image resolution	1280 × 1024 pixels
Shutter speed	1/5000 sec

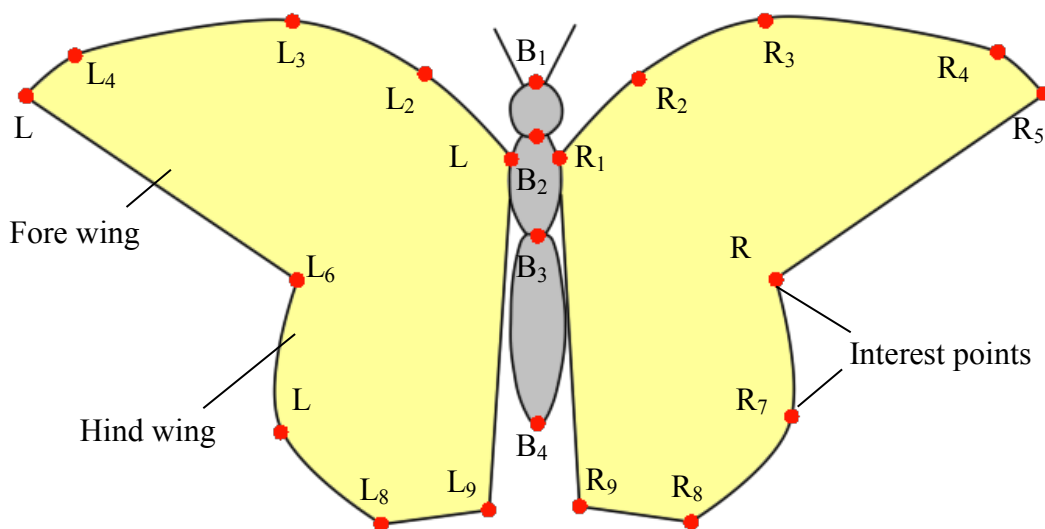


**Figure 2:** Interest points of body and wing.

Figure 2 shows the measured points of the butterfly. The body is divided into three parts: head, thorax, and abdomen ( $B_1$ - $B_4$  in Figure 2). The measurements of the wings are carried out along the edges since the opaque wings occlude points on the surfaces frequently during flight ( $L_1$ - $L_9$  and  $R_1$ - $R_9$  in Figure 2).

## 2.2 Definitions of the Parameters

To determine the attitude and flight parameters of a butterfly, we define the butterfly coordinate system  $\Sigma_B$  (Figure 3). The  $X_B$  axis is the vector from  $B_1$  to  $B_3$ . The  $Z_B$  axis is the vector product of the  $X_B$  axis and the body-span vector from  $L_1$  to  $R_1$ . The  $Y_B$  axis is the vector product of  $Z_B$  and  $X_B$ .

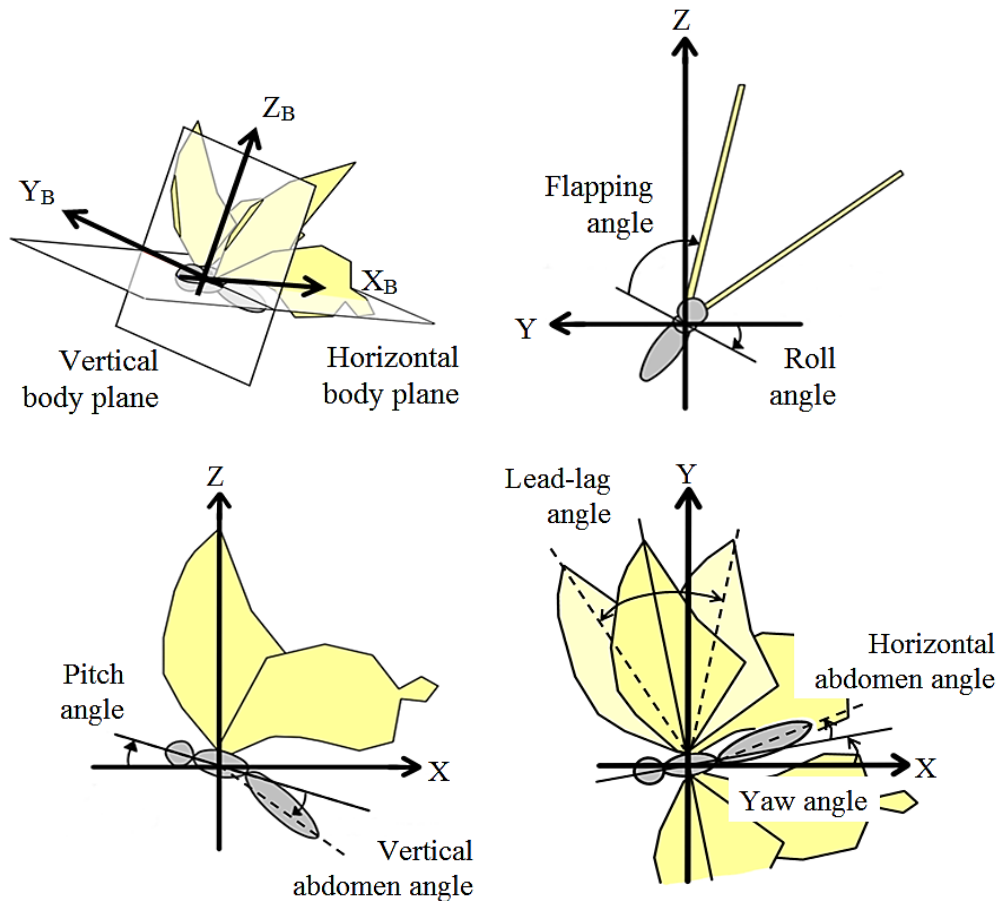


**Figure 3:** Definitions of the butterfly frame, angles, and posture.

The attitude of the butterfly is shown in Figure 3, in which the roll, pitch, and yaw angles are denoted by  $\phi$ ,  $\theta$ , and  $\psi$ , respectively. Here, we define horizontal and vertical body planes that have  $Z_B$  and  $X_B$  as normal vectors. The roll, pitch, and yaw angles are defined as follows:

$\phi$  is the angle between the horizontal body plane and the Y axis,  $\theta$  is the angle between the horizontal body plane and the X axis, and  $\psi$  is the angle between the vertical body plane and the Y axis.

The flight parameters describing the state of the butterfly are chosen as follows: The angle between the horizontal body plane and the normal vector of the fore wing is defined as the flapping angle. The flapping cycle is divided into two phases, up and down strokes. We also defined the lead-lag angle as a parameter which describes the wing state. The lead-lag motion of a butterfly controls not only the pressure center on the wings but also the wing area by overlapping the fore and hind wings (Fujikawa, 2008, 2010 and Udagawa, 2005). This motion is parameterized by the angle between the vertical body plane and the vector from the root to the tip of the wing. The parameter describing the state of the abdomen is as follows: A butterfly swings its abdomen horizontally and vertically as well as flapping. The vertical abdomen angle is defined as the angle between the horizontal body plane and the abdomen vector from  $B_3$  to  $B_4$ . The horizontal abdomen angle is the angle between the body and the abdomen vectors.

### 3. Computational Fluid Dynamics

#### 3.1 Boundary Conditions around a Butterfly

In this study, we analyzed the flow field around a real butterfly flying in the photographed space. Using the measured points and velocities defined in the previous section as the mesh boundaries, the behavior of real vortices can be visualized. The wing and body are divided into meshes bounded by the measured points (Figure 4). The leading edges of the fore wings ( $L_1$ - $L_5$  and  $R_1$ - $R_5$ ) and the side edges of the hind wings ( $L_6$ - $L_8$  and  $R_6$ - $R_8$ ) are approximated to match a butterfly wing shape using third order spline interpolation. The body and other wing sections are divided linearly. To simplify the calculation, our simulation considers the fore and hind wings as one. The body of the butterfly model is composed of three parts, head, thorax, and abdomen. These parts are cylindrical and their axes are the lines which join the measured points. The coordinates of the butterfly are obtained by image processing every millisecond using a 1000 frame per second camera. To improve calculation accuracy, we further divided these data intervals into 0.01ms periods through the natural third spline interpolation. The approximate curve is continuous up to second order.

### 3.2 Governing Equations of the Flow

The numerical solver in this study analyzes the air flow caused by the flapping motion of the butterfly using the measured points and velocities as the boundary conditions. The governing equations for CFD are the continuity equation and the Navier-Stokes equation. The flow is considered to be 3D, incompressible, and unsteady. In equation (1),  $U$ ,  $\rho$ ,  $P$ , and  $\mu$  are the mean velocity vector of flow, density, pressure, and the coefficient of viscosity, respectively.

$$\begin{cases} \nabla \cdot U = 0 \\ \frac{\partial U}{\partial t} + (U \cdot \nabla)U = -\frac{1}{\rho} \nabla P + \frac{\mu}{\rho} \nabla^2 U \end{cases} \quad (1)$$

Finite element method (FEM) was used for the calculation scheme. This method is stable and maintains high accuracy with large mesh deformation. The calculation space mesh tends to deform because the flapping range of a butterfly is far wider than that of other insects, at almost

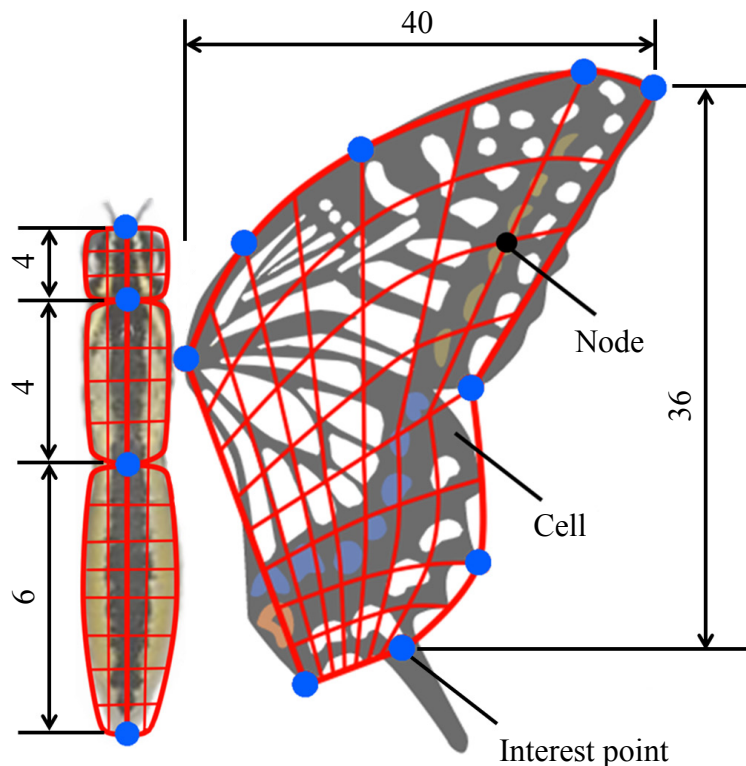


**Figure 4:** Meshing for CFD: division numbers of the body and wing.

180deg. Therefore, we adopt an arbitrary Lagrangian-Eulerian (ALE) method for the deformation and motion of the calculation space and butterfly meshes. The calculation of flow is stabilized using the stream-upwind/Petrov-Galerkin (SUPG) method. Dividing the

Navier-Stokes equation into two terms using a simplified marker and cell method (SMAC) method allows the explicit and implicit calculations of velocity and pressure, respectively.

The size of the calculation space is  $130 \times 100 \times 100 \text{cm}^3$  and the number of nodes for FEM is  $94 \times 108 \times 75$ . Figure 5 shows the boundary conditions of the space. Here,  $u_{body}$ ,  $v_{body}$ ,  $w_{body}$ ,  $u_{cal}$ ,  $v_{cal}$ , and  $w_{cal}$  denote the velocities of the butterfly and the wall. The origin of the coordinate system of the calculation space is fixed at the initial position of the thorax and the X axis points in the opposite direction to the butterfly's movement.

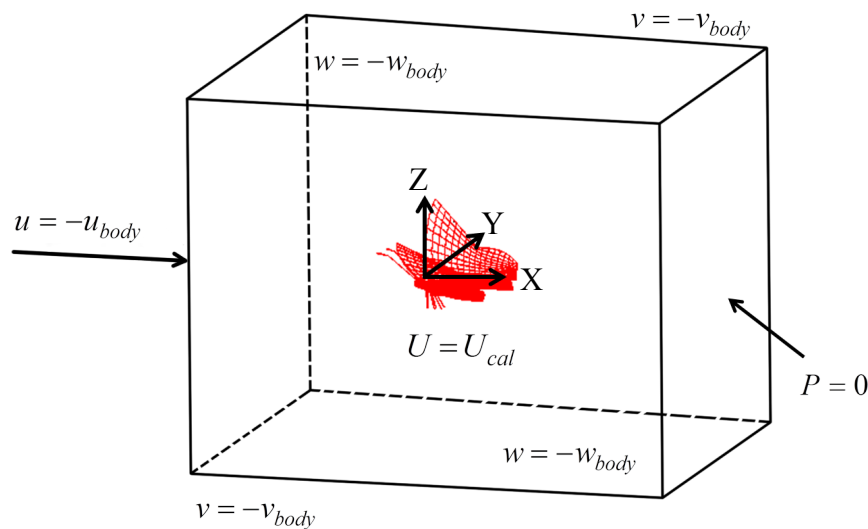


**Figure 5:** Calculation space and boundary conditions.

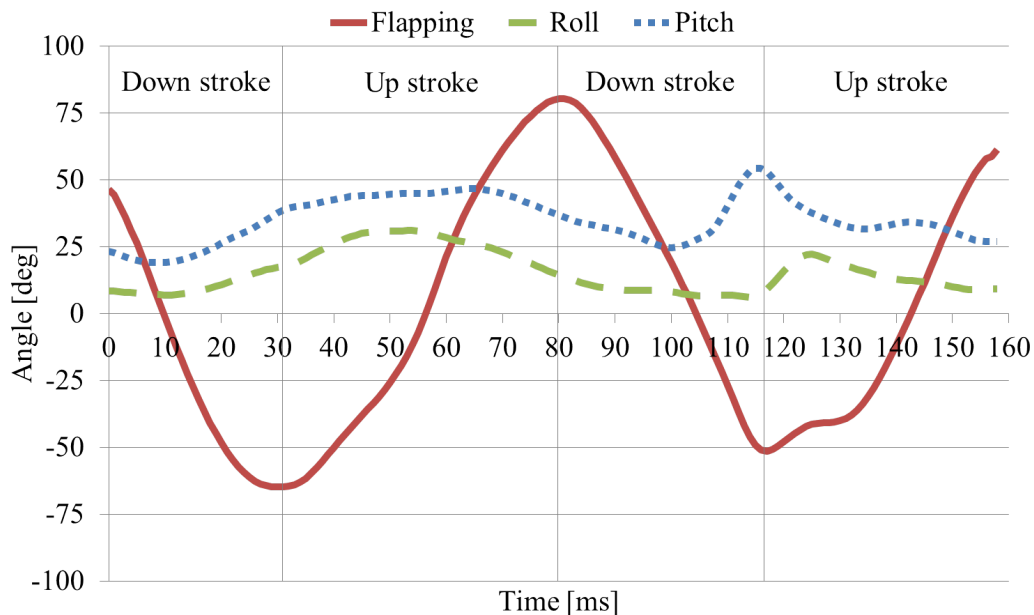
## 4. Computational Fluid Dynamics

We photographed two kinds of flight patterns in which the butterfly rotated around different axes, to clarify the butterfly's rotation mechanisms. Section 4.1 describes a pitch rotation which is a typical flight pattern for a butterfly. Section 4.2 describes a roll rotation and clarifies the attitude recovering mechanism for rotating from a rolled state to a horizontal state.

### 4.1 Flow Field of a Pitch Rotational Flight

In this section, we describe the typical pitch rotational flight pattern. The initial attitude of the butterfly was  $\phi = 1.5 \text{ deg}$ ,  $\phi = 23.4 \text{ deg}$ , and  $\phi = -2.8 \text{ deg}$ . Figure 6 shows the transitions of the flapping, pitch, and roll angles. It can be seen that the pitch angle increased simultaneously with the down stroke. The wing motion changed from the down stroke to the up

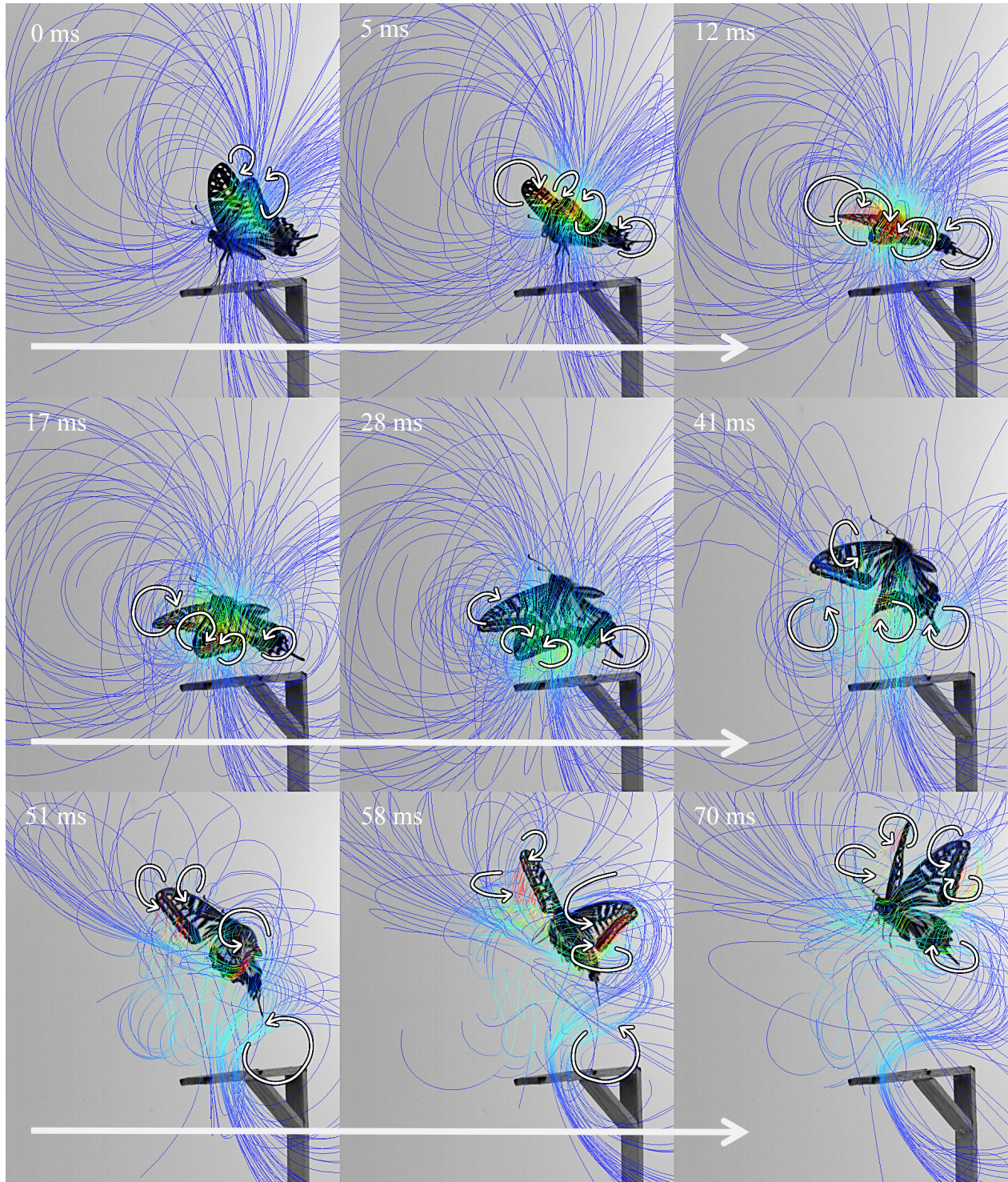
stroke at a flapping angle of  $-70$  deg. The pitch angle continued to increase for 10ms after the stroke reversal. The reaction force on the wing provided the thrust since the stroke was in the positive X direction. In the up stroke phase from 31ms to 81ms, the butterfly flew forward with decreasing pitch angle. The down stroke started again at a flapping angle of 80deg. As well as the first stroke, the pitch angle increased with a delay of 10ms in the second stroke. The roll angle was almost unchanged throughout the two flapping cycles. The maximal variation was 25deg at a flapping angle of  $-10$  deg during a first upstroke (Figure 6).



**Figure 6:** Time history of the angles: Pitch rotational flight.

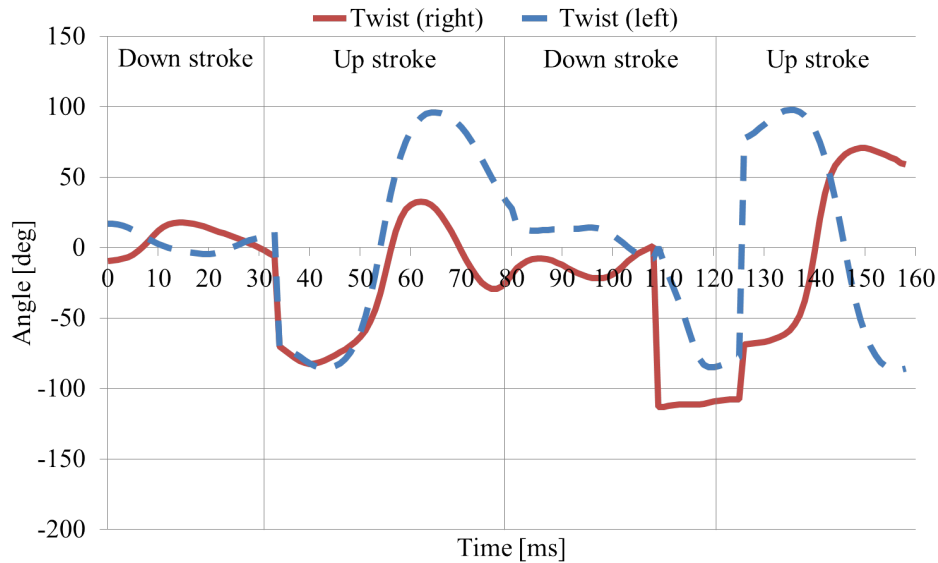
Figure 7 shows the streamlines around the wings caused by the flapping motion. The streamlines are colored according to the flow speed, where the red lines are faster and blue lines are slower. The leading-edge vortices (LEV) and wing tip vortices (WTV) which were present on the upper surface of the wing were generated during the down stroke. These vortices decrease pressure causing the differential pressure between the top and bottom surfaces of the wing. Dickinson *et al.* have reported the lift generation mechanisms (Dickinson, 1999), which are as follows. Rotational circulation means that the rotation of the wing at the time of the stroke reversal generates an upward force. The wake capture mechanism explains the increase in aerodynamic force during the stroke reversal. Figure 8 shows the twist angle of the left and right wings during two flapping cycles. It shows that the twist angle changed at the time of the stroke reversal. We think that the lift force was increased by rotational circulation at that time (Dickinson, 1999). The axes of the vortices are parallel to the wing surface.

Figure 9 shows the constant pressure surfaces on the wings as stroboscopic images. The red and blue surfaces show positive and negative pressures of 0.8Pa and  $-0.8\text{Pa}$ , respectively. The pressure is positive on the upper side and negative underneath during the down stroke. The



**Figure 7:** Stroboscopic images of streamlines: Pitch rotational flight.

butterfly rose with increasing pitch angle due to the differential pressure that concentrated near the leading-edge of the fore wings. The pressure is positive underneath the wings and negative



**Figure 8:** Time history of twist angles: Pitch rotational flight.

on the upper side during the up stroke. Similarly to the down stroke, the butterfly flew forward with decreasing pitch angle due to the differential pressure that concentrated near the leading-edge of the fore wings.

Figure 10 shows the time history of the reaction force on the left and right wings. During the pitch rotational flight pattern, the reaction forces of the left and right wings were changed in the similar tendency. The force on the right wing exceeded that on the left wing during the first down stroke. This continued until the upstroke at 46ms, at which time the roll angle also increased. From the start of the second flapping cycle, the reaction forces on the left and right wings were the same and the roll angle of the butterfly did not change.

## 4.2 Flow Field of a Roll Rotational Flight

This section describes the mechanism for rotating from a rolled state to a horizontal state. The initial attitude of the butterfly was  $\phi = -58.0$  deg,  $\theta = 52.1$  deg, and  $\psi = -87.8$  deg. Figure 11 shows the transition of the flapping, pitch, and roll angles. Unlike the previous flight pattern, the maximum variation in pitch angle was 25deg. The pitch angle decreased with the down stroke because the butterfly took off from the bottom side of the roost. The roll angle also decreased and the butterfly rotated around the roll axis in the clockwise direction.

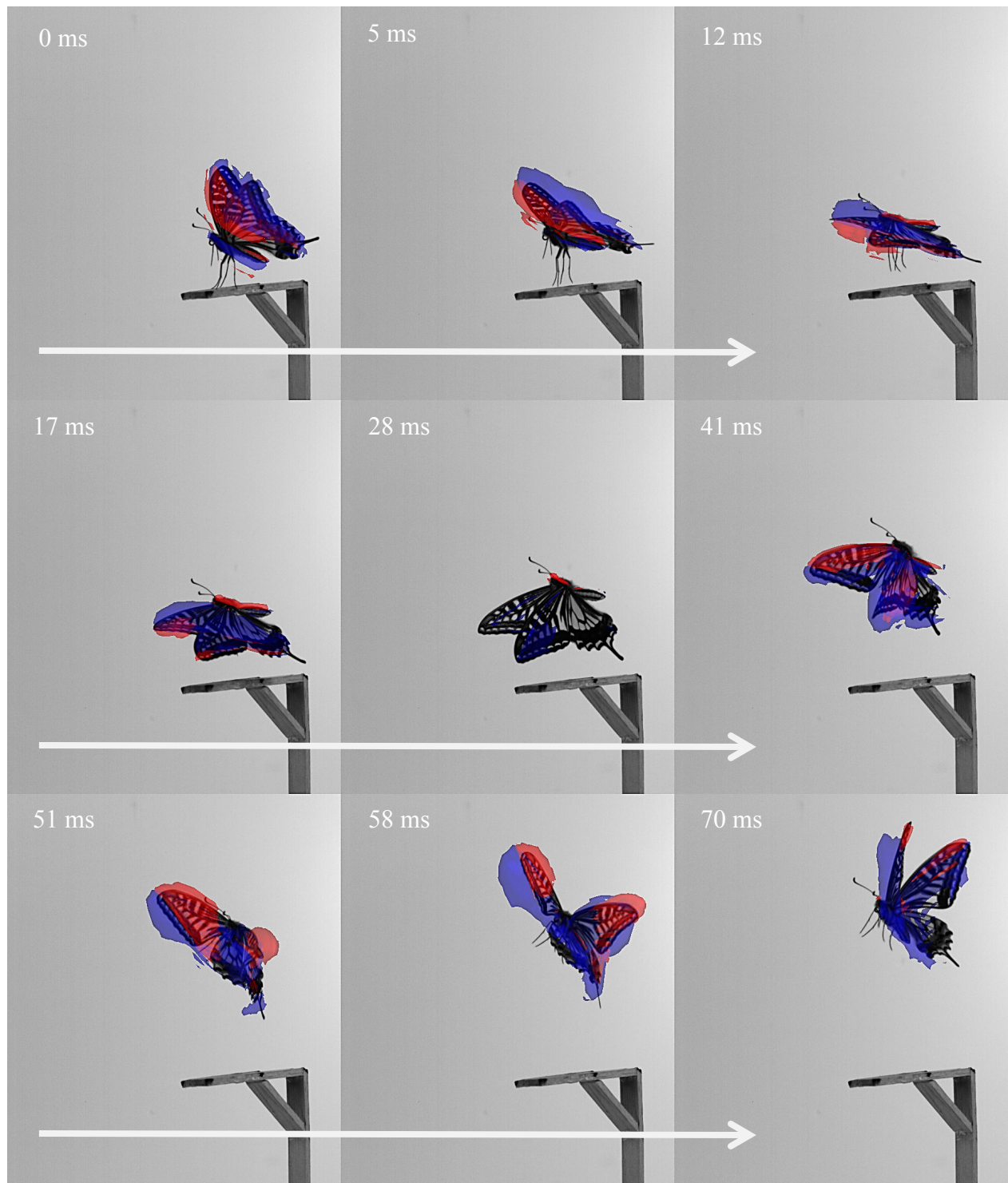


**Figure 9:** Stroboscopic images of the constant pressure surfaces: Pitch rotational flight.

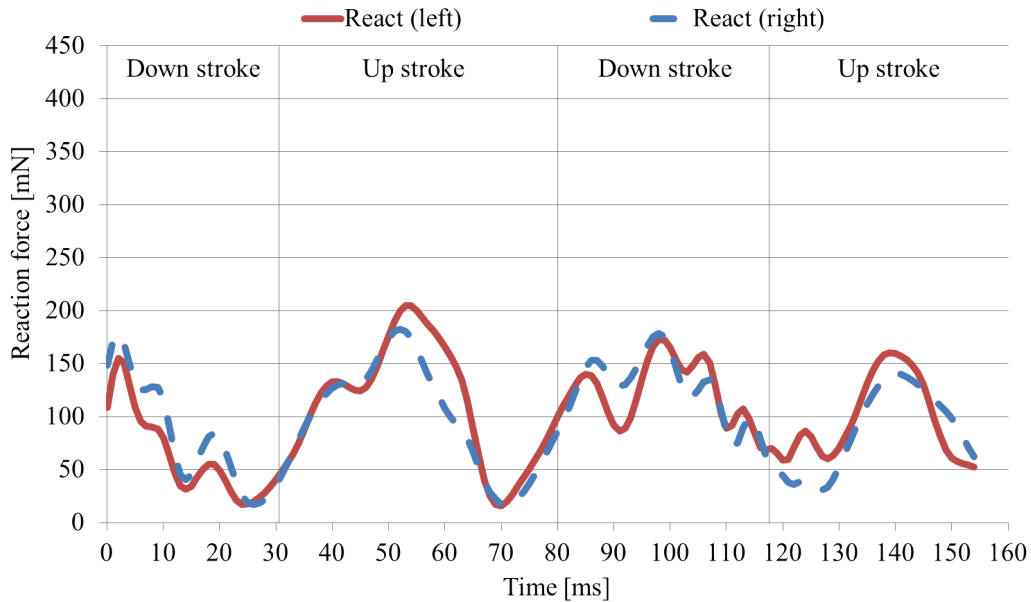


**Figure 10:** Time history of the reaction forces: Pitch rotational flight.

The reaction force acted in the negative X direction since the pitch angle was 50deg. The butterfly moved 5mm in the Z direction. The down stroke ended and the upstroke began at a flapping angle of -50deg. The pitch angle decreased for 10ms at the beginning of the upstroke. After that, it continued to increase until reaching a maximum at a flapping angle of 75deg. On the second down stroke, the flapping motion of the right wing preceded that of the left wing by 5ms. From this point the roll angle started to change. From 65ms, the rotational moment around the roll axis increased over 5ms because the direction of the reaction forces on the right and left wings were different.

Figure 12 shows the streamlines around the wing. The LEVs and WTVs, which were present on the upper surface of the wing, were generated during the down stroke, as in the pitch rotation maneuver. Figure 13 shows that the twist angle decreased from the beginning of down stroke and this angle also increased 10ms before the stroke reversal. We conclude that the butterfly, similarly to *Drosophila*, used rotational circulation by advancing the fore wing to the

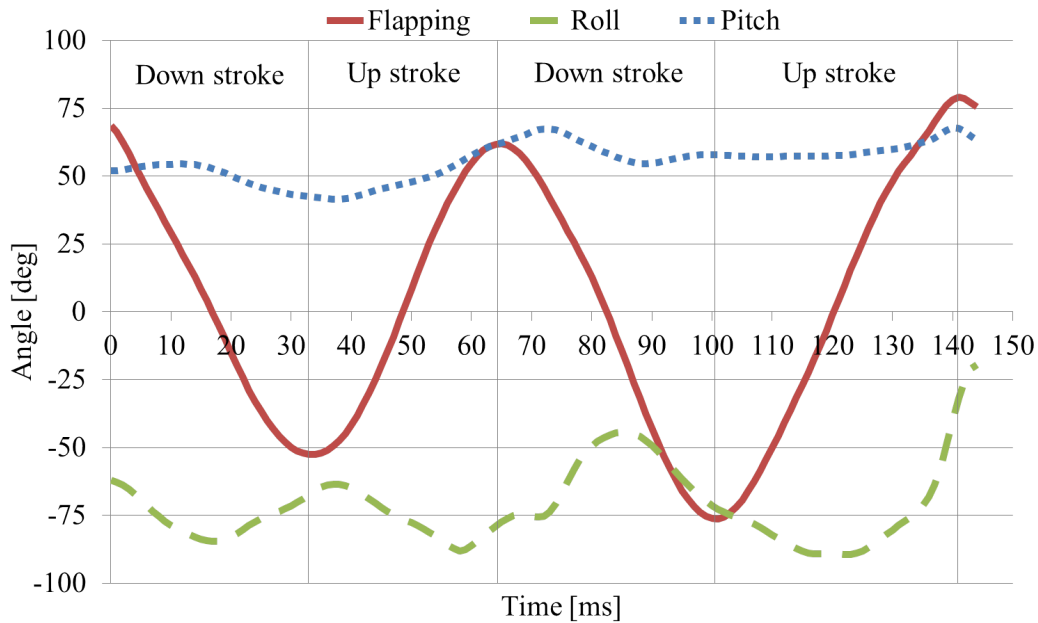


**Figure 11:** Time history of the angles: Pitch rotational flight.

hind wing (Dickinson, 1999; Lehmannl, 2005). The behavior of the vortices during the upstroke was different to that in the pitch rotation maneuver. In this case, the axis of the WTVs intersected the wings.

Figure 14 shows the constant pressure surfaces at the same time as those shown in Figure 12. The pressure distribution during the down stroke was similar to that in the pitch rotational flight pattern; however, that in the up stroke was different. The differential pressure during the up stroke concentrated near the leading-edges of the fore wings during the pitch rotation. In the roll rotation, however, it extended across the whole wing. The variation in pitch rotation was slight because the magnitudes of the reaction forces on the wings were equal. Figure 15 shows the time history of the reaction force on the wings. The reaction force on the right wing preceded that on left wing by 5ms when the second down stroke started. The butterfly rotated around the roll axis due to the angular moment generated. During the second down stroke, the maximal force on the right wing was 400mN, while that on the left wing was 220mN. The reaction force on the left wing was also larger than that on the right wing during the second up stroke. The roll attitude of the butterfly, which was initially roll-rotated at  $-58.0$  deg, became approximately horizontal at the start of the third down stroke.

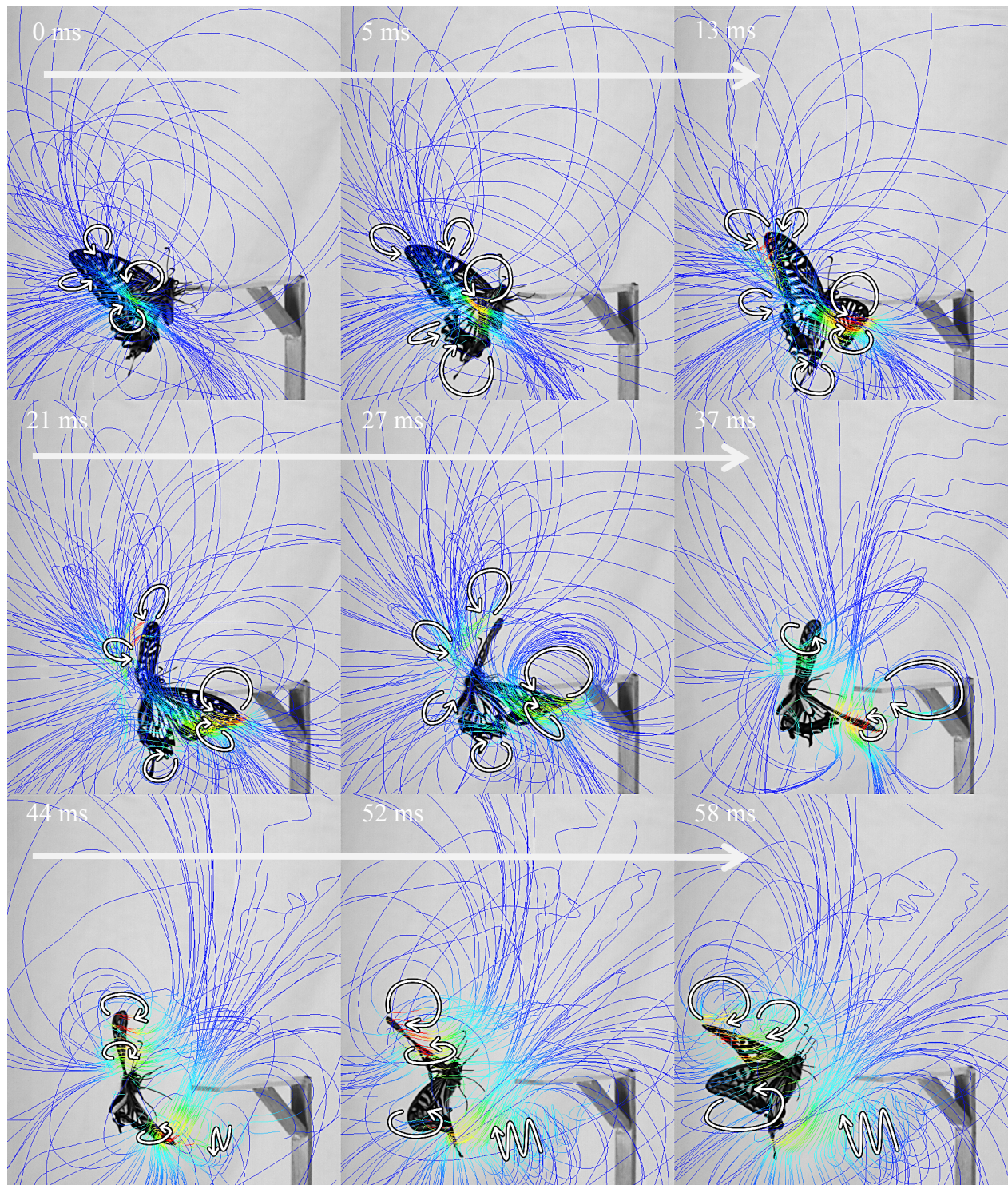


**Figure 12:** Stroboscopic images of streamlines: Roll rotational flight.

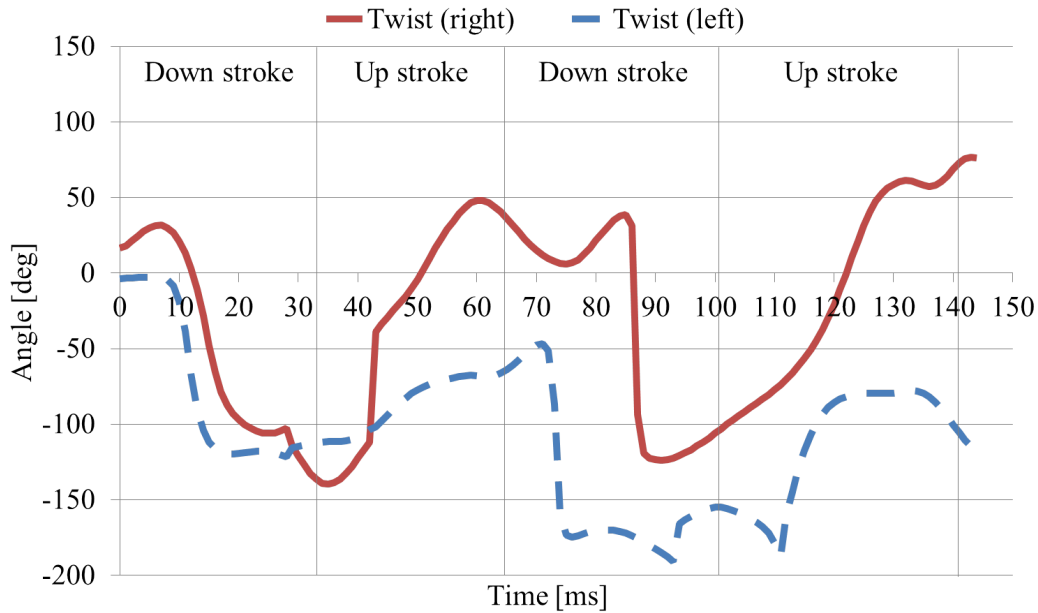


**Figure 13:** Time history of twist angles: Roll rotational flight.

## 5. Conclusion

In this paper, we analyzed vortices around the wings of a butterfly based on computational fluid dynamics using a three-dimensional high-speed camera information and clarified the posture control mechanism of a roll rotation. The results showed that the pressure distribution and behavior of the vortices changed according to the changes in attitude. In the case of a pitch rotational flight pattern, the pitch angle changed most significantly and the differential pressure concentrated near the leading edges of the fore wings. The maximum reaction force on both sides of the wing and the average angular moment about the pitch axis were 200mN and  $-32.0\mu\text{ Nm}$ , respectively. In the case of a roll rotational flight pattern, the roll angle changed most significantly and the differential pressure was distributed across the whole wing. The maximum reaction force on the left wing was 400mN and that on the right wing was 220mN. The differential force generated an angular moment about the roll axis, which was  $-282.0\mu\text{ Nm}$  on average during flight. These results show that a butterfly controlled its rotational direction by changing the pressure distribution.

In future work, we need to analyze the long-term flight to clarify the posture stabilization mechanisms and validate it by deriving the flight experiment of ornithopter.

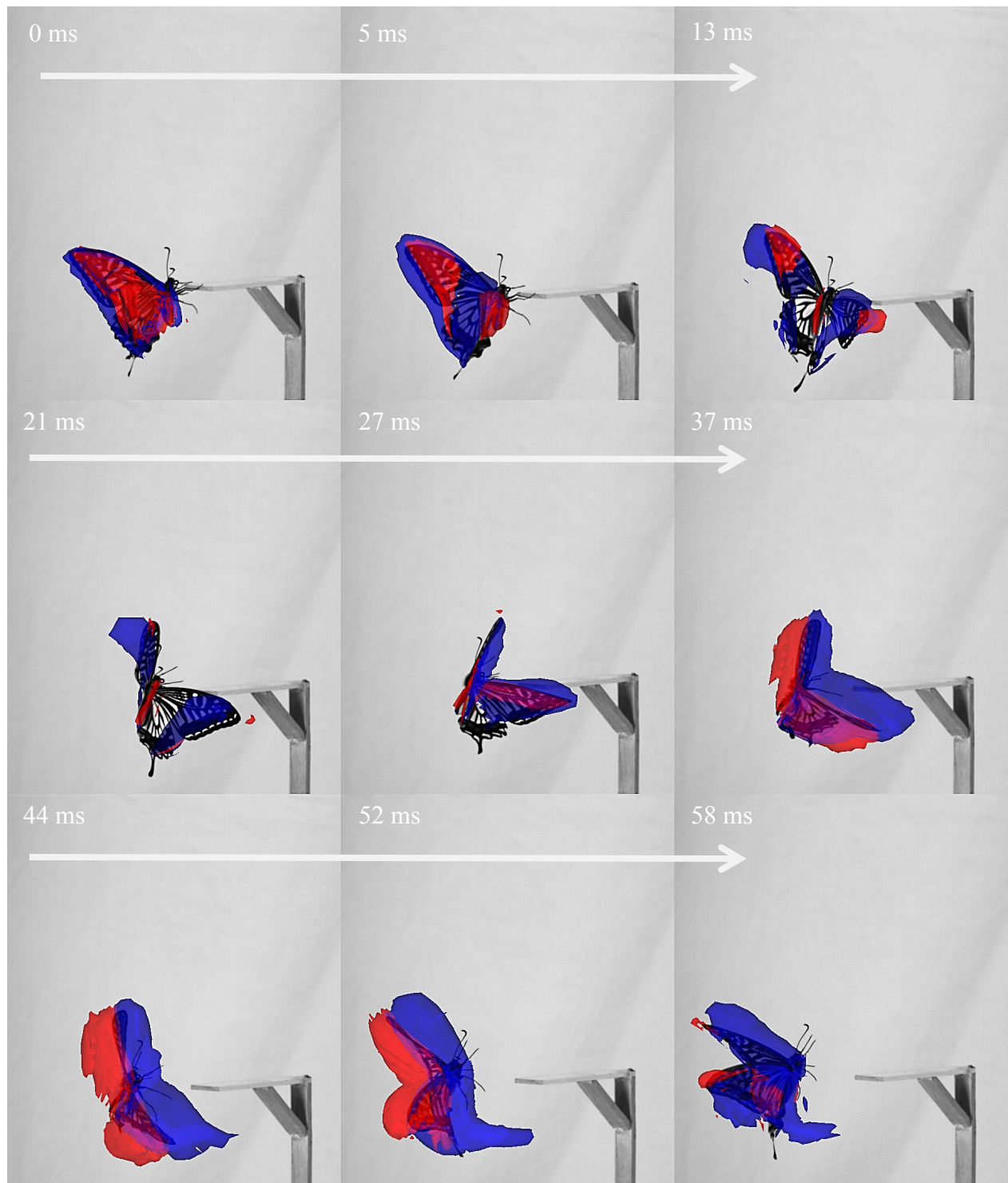


Figure 14: Stroboscopic images of the constant pressure surfaces: Roll rotational flight.

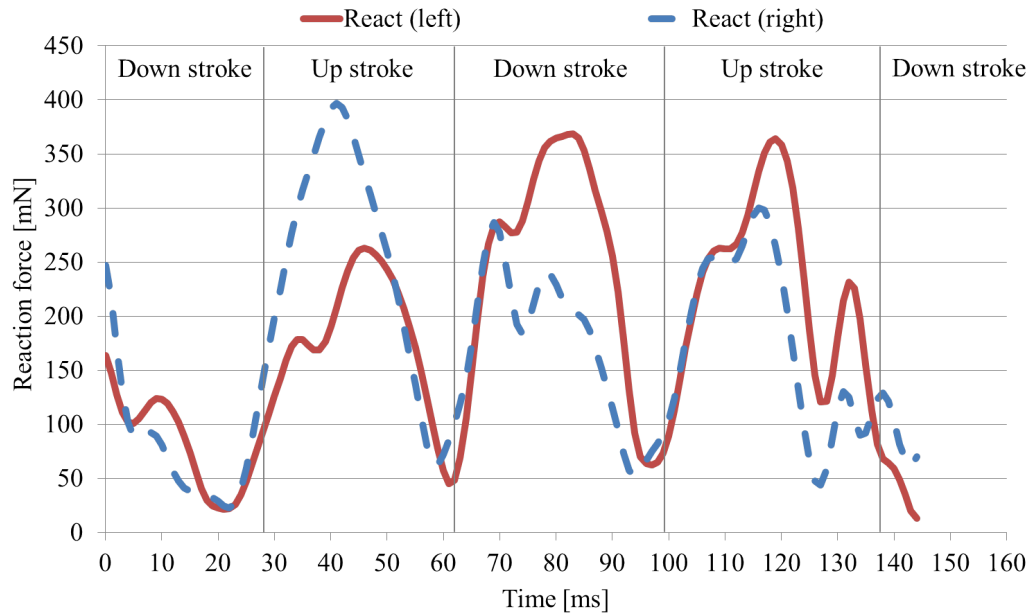


Figure 15: Time history of the reaction forces: Roll rotational flight.

## 6. References

- Nestor O. Perez-Arancibia, John P. Whitney, Robert J. Wood, (2011). Lift Force Control of a Flapping-Wing Micro Robot, American Control Conference, 4761-4768.
- Nestor O. Perez-Arancibia, John P. Whitney, Robert J. Wood, (2013). Lift Force Control of Flapping—Wing Micro Robots Using Adaptive Feed-forward Schemes, IEEE / ASME Transactions on Mechatronics, 155-168.
- Fu-Yuen Hsiao, Lung-Jieh Yang, Sen-Huang Lin, Cheng-Lin Chen, Jeng-Fu SHEN, (2012). Autopilots for Ultra Lightweight Robotic Birds—Automatic Altitude Control and System Integration of a sub-10g Weight Flapping-wing Micro Air Vehicle, IEEE Control Systems, 35-48.
- Takahashi, H., Matsumoto, K., and Isao Shimoyama. (2012). Differential Pressure Measurement of an Insect Wing Using a MEMS Sensor. International Conference on Complex Medical Engineering, 349-352.
- Fuchiwaki, M., Kuroi, T., Tanaka, K., and Tabata, T. (2013). Dynamic behavior of the vortex ring formed on a butterfly wing. Experimental in Fluid, 13-24.
- Fujikawa, T., Sato, Y., Yamashita, T., and Kikuchi, K. (2010). Development of A Lead-Lag Mechanism Using Simple Flexible Links for A Small Butterfly-Style Flapping Robot. WAC2010 (ICDES2005, MSSP2008, ISAC2010), 1-6.
- Fujikawa, T., Hirakawa, K., Okuma, S., Udagawa, T., Nakano, S., and KIKUCHI, K. (2008).

\*Corresponding author (Masahiro Shindo). Email address: [s1376014we@s.chibakoudai.jp](mailto:s1376014we@s.chibakoudai.jp).

©2014. American Transactions on Engineering & Applied Sciences. Volume 3 No. 4 ISSN 2229-1652 eISSN 2229-1660 Online Available at <http://TUENGR.COM/ATEAS/V03/0233.pdf>.

Development of a small flapping robot: Motion analysis during takeoff by numerical simulation and experiment. *Mechanical Systems and Signal Processing*, 22, 1304-1315.

Udagawa, T., Fujikawa, T., GAO, X., and Kikuchi, K. (2005). Development of a Small-Sized Flapping Robot. *The 1st international conference on design engineering and Science*, 283-288.

Dickinson, M., Lehmann, F., and Sane, S. (1999). Wing Rotation and the Aerodynamic Basis of Insect Flight. *Science*, 284, 1954-1960.

Lehmann, F., Sane, S., and Dickinson, M. (2005). The aerodynamic effects of wing-wing interaction in flapping insect wings. *The Journal of Experimental Biology*, 208, 3075-3092.



Masahiro Shindo is a graduate student of Department of Advanced Robotics, Chiba Institute of Technology, Japan. He received his degree in Engineering from Chiba Institute of Technology in 2013. He also received the Hatakeyama Award, the Japan Society of Mechanical Engineers in 2013. He investigates the flight mechanism of a butterfly using a three-dimensional computational fluid analysis and an insect-scale flapping robot.



Dr. Taro Fujikawa is an Assistant Professor of Department of Robotics and Mechatronics at Tokyo Denki University, Japan. He received his Ph.D. in Engineering from Chiba Institute of Technology, Japan, in 2011. From 2011 to 2012, he was a Postdoctoral Researcher at Research Institute of Chiba Institute of Technology. He was a recipient of the Miura Award, the Japan Society of Mechanical Engineers in 2007, and the Best Paper Award of the 1st International Conference of Design Engineering and Science (ICDES2005). His research interests include biomimetic robots, mobility vehicles, and mechanical engineering design.



Dr. Koki Kikuchi is a professor of Department of Advanced Robotics, Chiba Institute of Technology, Japan. He received his Ph.D. in Engineering from Tokyo University of Science in 1999. He also received the best paper award of the International Conference of Design Engineering and Science (ICDES2005) from Japan Society of Design Engineering, JSDE, and the best paper award of journal of JSDE. He investigates mechanisms creating insect abilities and develops small robots such as a butterfly-style flapping robot, vertical wall climbing robot, on-water running robot, etc. based on insect scale physics.

**Peer Review:** The original of this article has been submitted to The 3rd International Conference on Design Engineering and Science (ICDES 2014), held at Pilsen, Czech Republic. The Paper Award Committee of ICDES 2014 has reviewed and selected this paper for journal publication.